Ocean tidal solutions in Antarctica from GRACE inter-satellite tracking data

Shin-Chan Han,[1,2] Richard D. Ray,[1] and Scott B. Luthcke[1]

Received 31 July 2007; revised 4 September 2007; accepted 4 October 2007; published 10 November 2007.

[1] Long-wavelength components of the oceanic tides surrounding Antarctica are estimated directly from three years of GRACE satellite-to-satellite ranging measurements. An inversion is performed for the major constituents M_2, O_1, and S_2, with K_1 excluded because of inadequate phase sampling. The tides are parameterized as localized average mass anomalies over areas approximately 300^2 km^2; other parameters, including satellite state adjustments, are estimated simultaneously with the tides. Qualitative comparison of our solutions with in situ tide measurements shows agreement in spatial pattern, clearly indicating regions where our adopted prior model is inadequate. To exploit these solutions, follow-on work must assimilate these long-wavelength components into a high-resolution numerical tidal model. **Citation:** Han, S.-C., R. D. Ray, and S. B. Luthcke (2007), Ocean tidal solutions in Antarctica from GRACE inter-satellite tracking data, *Geophys. Res. Lett.*, *34*, L21607, doi:10.1029/2007GL031540.

1. Introduction

[2] Large-scale mass variations caused by terrestrial water, ocean, ice sheet, earthquake, and post-glacial rebound are among the primary applications of the satellite gravity mission, Gravity Recovery And Climate Experiment (GRACE) [*Tapley et al.*, 2004]. Owing to ongoing efforts to develop various post-processing techniques of monthly geopotential coefficients (see a review by *Kusche* [2007]) and further localized and direct analyses of satellite tracking data [*Rowlands et al.*, 2005; *Han et al.*, 2005], it is possible to determine mass variations with spatial resolution of ~400 km and temporal resolution of a month (with geopotential coefficients) and 10 days or even less (with satellite tracking data, depending on latitude). When the sought-after geophysical signals are dominated by long-term temporal variability (seasonal and interannual), such temporal resolutions are satisfactory, although improved spatial resolution is still desirable.

[3] The sub-daily mass variation associated with ocean tides is one of the most energetic time-variable gravity components. An a priori ocean tide model is typically applied to and removed from the GRACE measurements. Any imperfections in the ocean tidal modeling can yield spurious longer-term variability (some ten days to thousands of days) in monthly or sub-monthly mean gravity estimates via aliasing [e.g., *Ray and Luthcke*, 2006]. Such errors can mimic climate-related signals over a limited time span (e.g., K_1 tidal errors and inter-seasonal trends may appear similar over ~4 year periods). *Han et al.* [2005] noticed M_2 and S_2 errors in the CSR4.0 model [*Eanes and Bettadpur*, 1995] underneath the Antarctica Filchner-Ronne ice shelves in 5-day mean gravity estimates processed with 2 years of GRACE tracking data. Significant S_2 errors in southeast Asian seas have been reported when the FES2004 [*Lyard et al.*, 2006] tide model is employed for production of monthly time series of GRACE geopotential fields [e.g., *Schrama et al.*, 2007]. It is clear that GRACE is sensitive to ocean tide errors and therefore potentially offers valuable new tidal information in places, such as polar seas, where tidal measurements are lacking and models are unreliable.

[4] Rather than merely observing aliased (ocean) tidal errors in mean gravity solutions, this paper focuses on direct extraction of the tide signals from the GRACE range-rate measurements. Estimation of such sub-daily signals is possible because the tidal frequencies are known and the mass variability can be parameterized in terms of analytic functions (sinusoids) in an inversion of a long time series of GRACE measurements. Much like satellite altimetry, this approach allows estimation of formally undersampled signals. Unlike altimetry, however, GRACE is sensitive only to relatively long (spatial) wavelengths of the tide. A follow-on study will examine how such long-wavelength components can be assimilated into a high-resolution numerical tidal model.

2. Localized Analysis of Inter-satellite Tracking Data

[5] In order to assess internal consistency among various modern tide models in terms of what GRACE directly measures, we computed 24-hour dynamic arcs of the two GRACE satellites using GEODYN software [*Pavlis et al.*, 2006], following the methodology described in *Luthcke et al.* [2006]. We changed only the ocean tidal force components based on various models, keeping all other force models the same. We used four different ocean tide models: TPXO.6 [*Egbert and Erofeeva*, 2002], FES04 [*Lyard et al.*, 2006], GOT00 [*Ray*, 1999], and CSR4.0 [*Eanes and Bettadpur*, 1995]. For the solid Earth tides, we use the models according to the IERS Standards [*McCarthy and Petit*, 2004]. Computed dynamic arcs are consistent within ±10 mm and ±20 μm/s in position and velocity, respectively, for each individual satellite, thus indicating that tide model differences cause such level of differences in absolute (not relative) orbit components.

[6] Figure 1 presents model-induced differences in terms of range-rate along the computed GRACE trajectory at

[1]Planetary Geodynamics Laboratory, NASA Goddard Space Flight Center, Greenbelt, Maryland, USA.
[2]Goddard Earth Science and Technology Center, University of Maryland Baltimore County, Baltimore, Maryland, USA.

Copyright 2007 by the American Geophysical Union.
0094-8276/07/2007GL031540

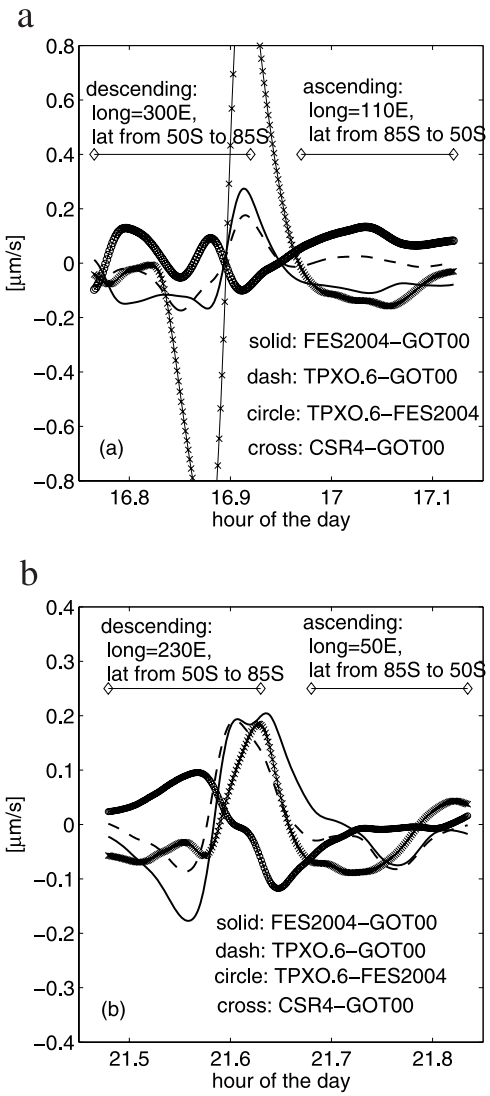

Figure 1. Inter-satellite range-rate perturbations caused by ocean tide modeling error. They are calculated from differences in various models including GOT00, TPXO.6, FES2004, and CSR4.0. (a) For the first half of period, the satellites overfly the Larsen and Ronne ice shelves at the longitude of 300°E in a descending direction. For the second half of period, they overfly the east Antarctic continent at the longitude of 110°E in an ascending direction. (b) The satellites overfly mostly the continental region except the Amundsen Sea at the beginning. The large perturbation exceeding ±1 μm/s in the difference of CSR4.0 and GOT00 is caused by the un-modeled tide beneath Filchner-Ronne ice shelves in CSR4.0 model. Besides CSR4.0 near the ice shelves, all tide models disagree by about ±0.2 μm/s perturbation along the GRACE satellite trajectory (450 km altitude and 220 km baseline).

450 km altitude with 220 km baseline distance, when the satellites overfly Antarctica. In Figure 1a, GRACE orbits are affected mostly by tidal mass variation in Larsen and Ronne ice shelves when they are orbiting toward the south pole and then by mass variation in east Antarctica continent when they are orbiting away from the pole. In Figure 1b, they are affected by the Amundsen Sea and west Antarctica continent and then east Antarctica (Queen Maud Land). The range-rate anomaly from the difference of CSR4.0 and GOT00 easily exceeds ±1.0 μm/s above the Ronne ice shelf. This large difference is due to the fact that the CSR4.0 model neglects the tidal signal underneath all Antarctic ice shelves. *Han et al.* [2005] discovered that large perturbations from GRACE data after correcting tides based on CSR4.0 are observed at the Filchner-Ronne ice shelves with particular frequencies corresponding to M_2 and S_2 alias frequencies. Although the other modern tide models do not have such large disagreement near the ice shelf regions (as found in CSR4.0), all tide models are still inconsistent yielding a few 0.1 μm/s perturbation in GRACE range-rate. A typical precision of GRACE KBR instrument is 0.2 μm/s in RMS sense that is estimated from post-fit residual analysis [*Luthcke et al.*, 2006]. The

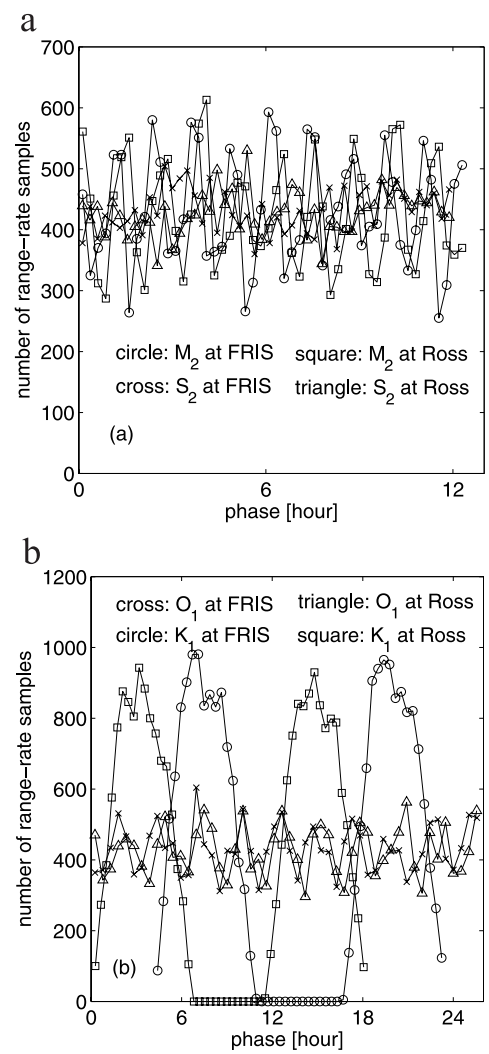

Figure 2. The numbers of GRACE range-rate data when the satellites overpass Filchner-Ronne ice shelves (80S–77S; 290E–320E) and Ross Sea (74S–71S; 180E–210E) in Antarctica, shown as a function of the phase of each tidal constituent, thus indicating how well GRACE samples each constituent. The K_1 tide at both locations is not sampled completely—merely less than 40% of its full cycle—even after 3 years of data.

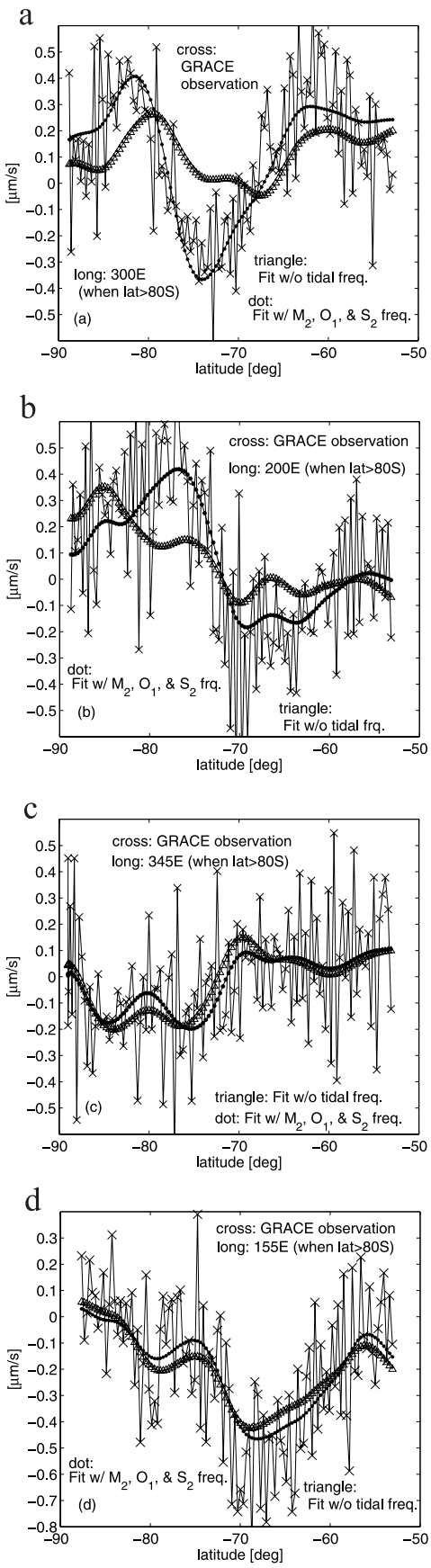

Figure 3. The actual GRACE measurements of inter-satellite range-rate with respect to a reference field. After inversions of the GRACE residual range-rate measurements with various parameterizations (including annual sinusoids with and without tidal sinusoids), the least-square solutions with tidal parameters more closely follow the observed range-rate perturbation when the tides are large at (a) Ronne ice shelf and Weddell Sea and (b) Ross ice shelf and Ross Sea. (c) and (d) The changes to the fit with the tidal parameters are small when the satellites go over mostly land.

detection of mass variability causing a few 0.1 μm/s (at most) can be possible since the tide is periodic phenomena and we can minimize random noise by using many GRACE observations.

[7] Tidal estimation requires sampling of some reasonable range of tidal phases for any desired constituent. Phase sampling is controlled fundamentally by the precession of the satellite orbit plane relative to the tide-raising body. Because the moon moves rapidly, all lunar tidal phases tend to be well sampled. But owing to GRACE's high inclination, and thus slow absolute precession rate, the sampling of solar tides can be problematic. In particular, the K_1 and K_2 tides need approximately 7 and 4 years, respectively, for complete phase sampling [*Ray and Luthcke*, 2006]. These statements are borne out in Figure 2, which shows the actual phase sampling of four major tidal constituents, as GRACE overflew two regions that include the Filchner-Ronne and Ross ice shelves. Three years of (almost) continuous GRACE data from July 2003 to June 2006 have been used. There are approximately 400 observations sampled at every phase of the constituents M_2, S_2, and O_1. However, more than half the phases for K_1 tide are not sampled, as expected from its aliasing period and our limited (3-year) observation period. Tidal solutions based on inadequate sampling are generally unreliable, and consequently we analyze only M_2, S_2, and O_1 constituents from the current GRACE data.

[8] The temporal variation of mean mass in each grid occupying equal area (220^2 km^2 when latitude below 80°S and 330^2 km^2 otherwise) is modeled by analytic functions including offset, linear trend, annual sinusoids (accounting mostly for climate signals), and various tidal sinusoids. Following the non-linear observational equation of surface mass anomaly and range-rate residual data derived by S.-C. Han et al. (Localized analysis of satellite tracking data for studying time-variable Earth's gravity fields, submitted to *Journal of Geophysical Research*, 2007), we estimate the respective coefficients of the modeled analytic functions for mass variation and initial state parameters of each overpass arc simultaneously using three years of GRACE data. Owing to the large number of observations and parameters, we divide Antarctica into three patches including the Weddell Sea, Ross Sea, and Amery ice shelf, and we solve for the parameters separately in each region. The spatial distribution of surface mass points is depicted in Figure 4.

[9] Figure 3 shows GRACE observations of *residual* range-rate after removing the calculated range-rate (based on GOT00 for ocean tide force component and other a priori force models as described by *Luthcke et al.* [2006]) along the computed orbits above various areas in Antarctica. Note

that the effect of imperfect orbits of two satellites to register the range-rate observations is negligible since the calculated orbits are typically as good as a few cm in position accuracy. As a test case, we consider the annual sinusoids, linear trend and offset in each grid on the surface as our parameters to be determined and estimate the corresponding coefficients directly from three years of GRACE range-rate residual data. Note that there are also arc-dependent parameters (initial relative state vectors) estimated simultaneously, as mentioned previously. Figure 3 shows the least-squares fit to the observations from the estimated mass coefficients of the analytic model excluding tidal frequencies and the estimated initial state. There are significant misfits (between triangle and cross in the figure) at Ronne and Ross ice shelves shown in Figures 3a and 3b that can be explained mostly by mis-modeling of the applied temporal behaviors and inherent error in the observations. We expand the analytic model for time-variation by adding three tidal frequencies M_2, S_2, and O_1 because they are the most energetic and estimable constituents from three years of data, as discussed. After the inversion with these six additional parameters at each grid, the least-squares fit is much improved and better follows the observations in both areas. Most of the systematic disagreements shown around the places like Ronne and Ross ice shelves such as in Figures 3a and 3b have disappeared and a random pattern dominates the remaining misfits. The difference of the two least-squares fits represents the effect of mis-modeled tidal mass variations and is shown to be within a few 0.1 μm/s, which is the predicted range of the modern tide model errors (Figure 1). However, the effects due to tidal parameters are small for the data overpassing mostly continental regions as shown in Figures 3c and 3d, implying smaller tidal signals on the surface around this region.

[10] We have made two additional least-square solutions with variations in adopted parameters including only M_2 sinusoids and only O_1 sinusoids to describe ocean tide. The RMS of post-fit residuals from the various solutions including (1) three constituents; 2) only M_2; and 3) only O_1 are 0.213, 0.217, 0.221 μm/s, respectively, over Weddell Sea, and 0.216, 0.222, and 0.219 μm/s, respectively, over Ross Sea. M_2 is more effective than O_1 in modeling the GRACE data over the Weddell Sea and vice versa over Ross Sea. This is consistent with the known tidal characteristics of these seas: diurnal tides dominate in the Ross Sea while semidiurnal tides dominate in the Weddell Sea (although with an amphidrome near the ice-shelf front) [e.g., *Padman et al.*, 2002].

3. Large Scale Tide Estimates and Ground Measurements

[11] In a standard form, we express the tidal height variation averaged over each grid element as $A_i f(t)\cos(\omega_i t + u(t) - \varphi_i)$, where A_i, φ_i, and ω_i are amplitude, phase lag, and frequency of a tidal constituent i, and $f(t)$ and $u(t)$ are time-dependent corrections accounting primarily for motion of the moon's node and perigee. The unknown parameters to be determined are A_i and φ_i for each constituent.

[12] We initially model tidal parameters (6 sinusoids corresponding to M_2, S_2, and O_1 frequencies) on both ocean (including ice shelf) and land. The estimated coefficients of the tidal frequencies in land areas are verified to be relatively small ($\sim$1 cm or less) except the land area close to coastlines and grounding lines where tidal signals leak in from the ocean or ice shelf. To obtain a more realistic solution (and also to facilitate later assimilation), we apply zero tide constraint to the land grid (defined as the grid showing 70% or greater land occupancy) in the least-squares inversion.

[13] The estimated tidal mass variations require independent assessment against external data. For this we adopt a number of in situ tidal estimates previously made by tide gauges, gravimeters, or GPS receivers. However, quantitative comparison between the satellite gravity estimates and these ground measurements is not straightforward, because the spatial resolution is significantly mismatched between the two measurements, i.e., a few hundred-km square averages versus point-wise variations. This is particularly true in a region such as Antarctica where the ground measurements are extremely sparse so that any further spatial filtering of ground data to mimic the satellite resolution is prohibited. Consequently, our comparison is limited to qualitative assessments against the ground measurements. Our ground data are extracted mainly from a compilation by *King and Padman* [2005]. We have selected data primarily in those locations where our satellite solutions indicate large anomalies. Unfortunately, there are no available ground data over the central Larsen Ice Shelf.

[14] Figure 4 shows $A_i \cos \varphi_i$ and $A_i \sin \varphi_i$ of M_2, S_2, and O_1 estimated from three years of the GRACE data inversion, relative to our applied prior model GOT00. Also shown are the comparison stations, also with respect to GOT00. Note that most of the GRACE estimates are within the depicted scale bar while some of the ground measurements exceed the scale bar and those are depicted as maximum or minimum value of the scale bar.

[15] M_2 estimates (with respect to GOT00) are greatest in magnitude in the Weddell Sea, as large as 20 cm near the grounding line. The sign of the cosine component at Filchner-Ronne ice shelves and the northern Weddell Sea are opposite. The signs of the sine component at George VI ice shelf (72°S, 68°W) and at Ronne ice shelf are the same, but the opposite with the ones at Filchner (80°S, 40°W), Brunt (75°S, 25°W), Riiser-Larsen (73°S, 15°W) ice shelves. The opposite signs of the sine components at the sea side and land side on Ross ice shelf are found. These features are observed in GRACE tide estimates and ground measurements. The M_2 tide on Larsen ice shelf shows a significant anomaly in GRACE, but it cannot be verified because of lack of ground data. The M_2 signal in GRACE is weak at Amery ice shelf but the negative sign in the cosine component still agrees with the ground data.

[16] Around Ross Sea and ice shelf, O_1 is the strongest component among the three constituents under our consideration. GRACE shows its dynamic change in sign from the grounding line toward the sea which agrees with the ground observations. It is interesting that the east and west sides of Ross ice shelf have fairly strong remaining signal with opposite sign in the sine component. While the cosine components in Ronne ice shelf and George VI ice shelf are of opposite sign, the sine components are of the same sign. All of them can be seen in both GRACE estimates and

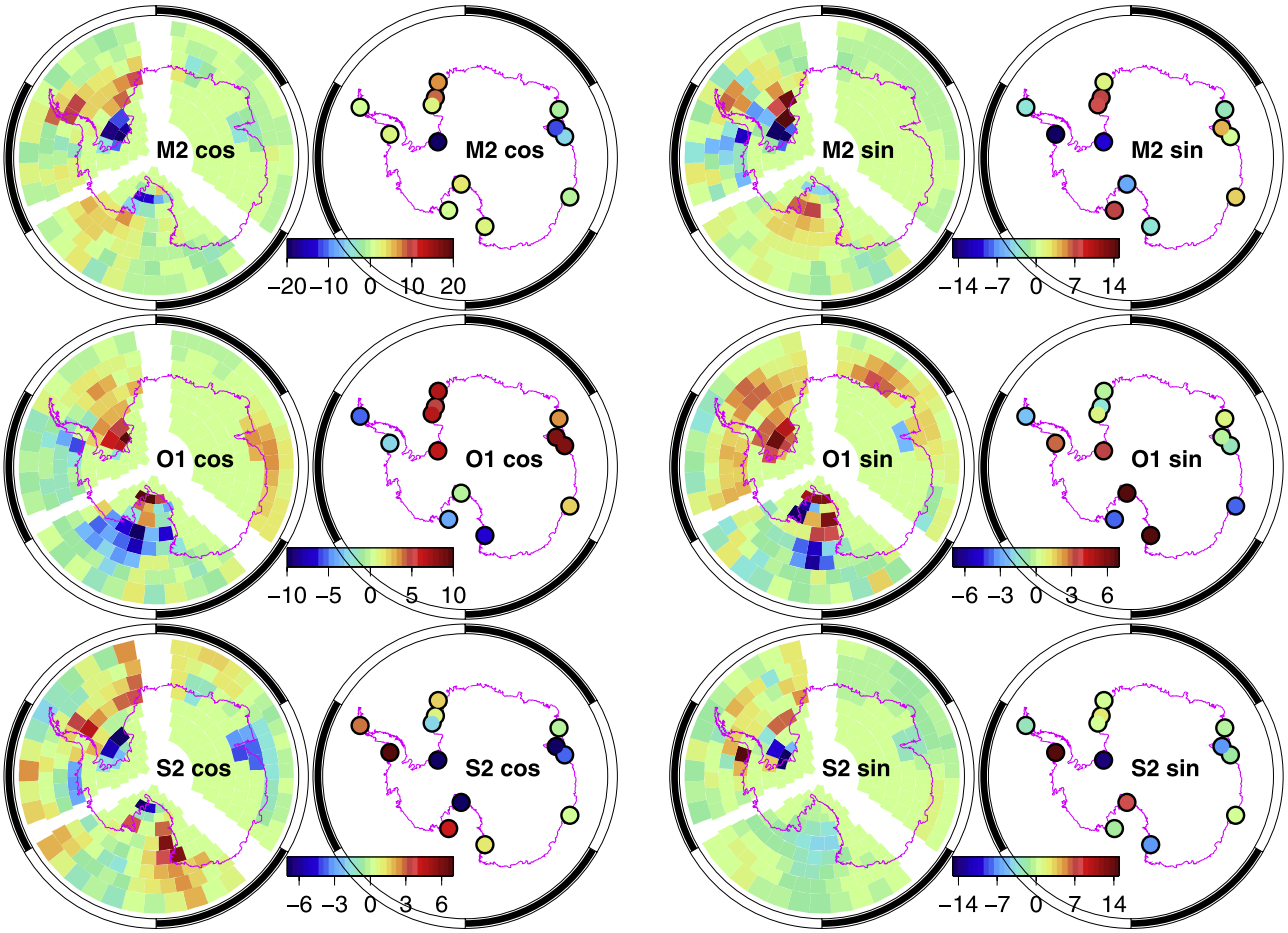

Figure 4. GRACE tidal solutions and ground data with respect to GOT00 model in cm for M_2, O_1, and S_2 constituents. Three years of GRACE range-rate residuals have been used to solve these coefficients of tidal sinusoids. The panels also show the spatial distribution of the equal-area grid on the surface where the time-variable mass is estimated by analytic parameterization. Note that the grid dominated by land has been constrained to have no tidal variation.

ground data. The positives in the cosine component around the Amery ice shelf and neighboring sea are also in agreement with the ground data. In addition, GRACE estimates indicates additional signal in Lützow-Holm Bay (70°S, 40°E) and Princess Ragnhild coast (70°S, 25°E) in the sine component that is not noted by any ground data.

[17] The most interesting feature found from the S_2 estimates and ground data is the one in George VI ice shelf, which is as large as 15 cm and behaves oppositely to the variation at Ronne ice shelf. Also there are moderate signals underneath the Amery ice shelf predicted from both GRACE estimates and ground data.

4. Remark

[18] We find the tidal solutions of M_2, S_2, and O_1 from three years of GRACE inter-satellite tracking data are in good qualitative agreement with sparse ground measurements at several locations in Antarctica. Owing to the mismatch in spatial resolution between our solutions and the ground point measurements, more quantitative comparisons must await assimilation of our long-wavelength solutions into high-resolution numerical tidal models. Only then can the full power of these solutions for improving tidal mapping be assessed and fully exploited. Although these GRACE solutions have limited spatial resolution, they are homogeneous in accuracy, resolution, and coverage over the entire Antarctic, a region that suffers from a severe lack of high-quality measurements. As the GRACE time series lengthens, we anticipate tidal solutions to improve and also to extend to more constituents, including the lunisolar diurnal tide. This should enhance other GRACE applications, including a more reliable estimation of inter-seasonal climate signals. We further anticipate future assimilation work to improve tide models by constraining long-wavelength components with these first-ever gravimetric estimates uniformly covering Antarctica from space.

[19] **Acknowledgments.** This work was supported by the U.S. National Aeronautical and Space Administration GRACE project. We acknowledge the NASA/GFZ GRACE project for the GRACE data products (distributed by JPL PODAAC). We acknowledge colleagues at JPL for producing the high-quality Level-1B GRACE products.

References

Eanes, R., and S. Bettadpur (1995), The CSR 3.0 global ocean tide model, *Tech. Memo. CSR-TM-95–06*, Cent. for Space Res, Univ. of Tex. at Austin, Austin.

Egbert, G. D., and S. Y. Erofeeva (2002), Efficient inverse modeling of barotropic ocean tides, *J. Atmos. Oceanic Technol.*, *19*, 183–204.

Han, S.-C., C. K. Shum, and K. Matsumoto (2005), GRACE observations of M_2 and S_2 ocean tides underneath the Filchner-Ronne and Larsen ice

shelves, Antarctica, *Geophys. Res. Lett.*, *32*, L20311, doi:10.1029/2005GL024296.

King, M. A., and L. Padman (2005), Accuracy assessment of ocean tide models around Antarctica, *Geophys. Res. Lett.*, *32*, L23608, doi:10.1029/2005GL023901.

Kusche, J. (2007), Approximate decorrelation and non-isotropic smoothing of time-variable GRACE-type gravity field models, *J. Geod.*, doi:10.1007/s00190-007-0143-3, in press.

Luthcke, S. B., D. D. Rowlands, F. G. Lemoine, S. M. Klosko, D. Chinn, and J. J. McCarthy (2006), Monthly spherical harmonic gravity field solutions determined from GRACE inter-satellite range-rate data alone, *Geophys. Res. Lett.*, *33*, L02402, doi:10.1029/2005GL024846.

Lyard, F., F. Lefèvre, T. Letellier, and O. Francis (2006), Modelling the global ocean tides: Insights from FES2004, *Ocean Dyn.*, *56*, 394–415.

McCarthy, D., and G. Petit (Eds.) (2004), *IERS Conventions [2003]*, *IERS Tech. Note 32*, 127 pp., Bundesamts für Kartogr. und Geod., Frankfurt am Main, Germany.

Padman, L., H. Fricker, R. Coleman, S. Howard, and L. Erofeeva (2002), A new tide model for the Antarctic ice shelves and seas, *Ann. Glaciol.*, *34*, 247–254.

Pavlis, D. E., S. Poulose, and J. J. McCarthy (2006), *GEODYN Operations Manuals*, SGT Inc., Greenbelt, Md.

Ray, R. D. (1999), A global ocean tide model from TOPEX/POSEIDON altimetry: GOT99.2, *NASA Tech. Memo., 1999–209478*.

Ray, R. D., and S. B. Luthcke (2006), Tide model errors and GRACE gravimetry: Towards a more realistic assessment, *Geophys. J. Int.*, *167*, 1055–1059, doi:10.1111/j.1365-246X.2006.03229.x.

Rowlands, D., S. Luthcke, S. Klosko, F. Lemoine, D. Chinn, J. McCarthy, C. Cox, and O. Anderson (2005), Resolving mass flux at high spatial and temporal resolution using GRACE intersatellite measurements, *Geophys. Res. Lett.*, *32*, L04310, doi:10.1029/2004GL021908.

Schrama, E. J. O., B. Wouters, and D. A. Lavallée (2007), Signal and noise in Gravity Recovery and Climate Experiment (GRACE) observed surface mass variations, *J. Geophys. Res.*, *112*, B08407, doi:10.1029/2006JB004882.

Tapley, B. D., S. Bettadpur, J. Ries, P. Thompson, and M. Watkins (2004), GRACE measurements of mass variability in the Earth system, *Science*, *305*, 503–505.

S.-C. Han, S. B. Luthcke, and R. D. Ray, Planetary Geodynamics Laboratory, Code 698, NASA Goddard Space Flight Center, Greenbelt, MD 20771, USA. (schan@puuoo.gsfc.nasa.gov; sluthcke@puuoo.gsfc.nasa.gov; ray@nemo.gsfc.nasa.gov)